Chapter-IV

Sustainable lubricant additives based on castor oil and α-pinene

2.4.1 Introduction

The last few decades were the era for rapid progresses in science and technology. Their fast progresses have also augmented the production of synthetic materials globally every year. Among these materials, lubricants constitute a very large fraction. They are largely a mixture of a base oil and an additive.[1] The additives blended in the base oil have a wide variety of functions to deliver. They commonly are merged together as viscosity index improvers (VII) to bring about a variation in the viscosity index, to alter the low temperature fluidity as pour point depressants (PPD) and to keep many other parameters of the base stock to a satisfactory level.[2,3]

Though quite a large number of additives have been formulated to specialize the new age lubricants, the poly acrylate and poly methacrylate based additives are still in use in massive amount.[4] As a matter of fact, improvements of new age equipments are now indispensable without modern lubricant technology. Millions of tons of lubricants are produced every year to satisfy the mounting pressure from equipment manufacturers. It is estimated that about 40 million tons of lubricants are consumed globally every year.[5]

The present day lubricants are derived predominantly from petroleum base stocks and given their extensive carcinogenicity and toxicity, they are considered as potential soil and water pollutants. The problem even becomes graver when these petroleum-based products somehow enter the biosphere. It is argued that approximately 40% of these lubricants produced globally are reintroduced to the atmosphere annually through various non recoverable usages like refinery processes, urban runoff, industrial and municipal waste, accidental spillage etc.[6] This can have severe biological effects

with the potential to destroy the biota locally. Several research groups reported the pernicious effects of mineral oils on the atmosphere.[7,8]

Besides, with the rising demand of energy and the stock of fossil fuels declining all over the globe, there is an imperative need to explore some alternative biocompatible lubricants. In this investigation, lubricants derived from plant oils and their derivatives have gathered keen attention as an alternative to petroleum-based product and as a next generation lubrication solution. Even the escalating prices of mineral oils as compared to the plant oil in different parts of the world have forced to identify plant oils as a potential candidate for environment compatible lubricants. In addition to biocompatibility, these oils also have several other technical features that are ideal for their use in industrial application. With the high molecular mass of the triglyceride present in plant oils, they have a very little volatility and a nominal alteration in viscosity with temperature. The additive molecules and polar contaminants are also highly soluble in these plant oils.[9]

Unfortunately, plant oils also experience some of their inherent shortcomings. The bisallylic protons of the triglycerides are very prone to radical attack and therefore undergo oxidative cleavage to form polar oxy compounds.[10] The compounds so formed eventually results in insoluble deposit and enhance the viscosity of the oil. These shortcomings have, therefore, limited their market share globally to about only about 1%.[11] Thus, to compete with petroleum based oils and to bring resurgence in their market share, the disadvantages that are present in these vegetable oils must be removed without compromising their excellent tribological and environmentally relevant properties. One possible answer to this is to provide more stability by reducing or eliminating the unsaturation present in the triglyceride structures of vegetable oils with polymerisation or to blend it with some more stable alternatives.

Moreover, in order to retain the biocompatibility of the final lubricant formulation, the additive in the lubricants must also be biodegradable. The lubricant and the additive industries have been working together in this direction to develop environmentally friendly green products. Some research groups have reported the use of plant oil derivatives as a base fluid and, therefore, a combination of plant oil based additives and a base fluid derived from plant oil can act as a valuable alternative to petroleum based products and incur biodegradability to it.[6,12] Bio lubricants are considered as the lubricants of future and with over 100 species of tree born oil seeds available in India, it possess a great potential for production of bio lubricants from this seeds.[13] As reported by the Food and Agriculture Organization of the United Nations (FAO), India is among the world's largest producer of castor beans. Castor oil or its derivatives have been exploited broadly in the formulation of several products like feedstock for fuels, various functional fluids, reactive components of paints, coatings, polymers, process oils and base oil for lubricants.[14] Hence, due to its unique oleo chemical properties and in view of synthesizing new eco-friendly bio-additives, castor oil was chosen here. Again, α-pinene is a commonly seen terpenoid found in nature. It is a compound of the oils and resins of many species of coniferous trees especially the pine. It is also found in the oil of rosemary. In this study, homopolymer of castor oil and its copolymers with different proportion of α-pinene were produced. Their additive performances as VII and PPD were investigated through standard ASTM techniques for the base oils under examination. Besides, biodegradability of the synthesized polymers was also examined to assess their environmentally benign nature.

2.4.2 Experimental section

2.4.2.1 Materials

Castor oil (CO) was collected from a local grocer's shop and α-Pinene (GC 98 %) was purchased from Acros Organics (India). The solvent, toluene (GC 99.5%), was obtained from Merck Specialties Pvt., Ltd., (India). Methanol (GC 99.8%) was obtained from Thomas Baker Chemicals Pvt., Ltd., (India). Azobisisobutyronitrile (AIBN, GC 98%, to be used as an initiator) was purchased from Spectrochem Pvt., Ltd., (India) and was recrystallized from $CHCl_3$–CH_3OH before use. The rest of the chemicals were used as obtained without further purification. The fungal specimen was collected from the Department of Microbiology, North Bengal University, West Bengal, India. The two mineral base oils (BO1 and BO2) were kindly supplied by Indian Oil Corporation Ltd. (IOCL), India. The physical properties of the base oils are shown in Table 2.4.1 and the fatty acid composition of castor oil is shown in Table 2.4.2.

2.4.2.2 Preparation of the homopolymer and copolymers

Preparation of the homopolymer of castor oil (HCO) and its copolymer with α-pinene in three different concentrations [5%, 7.5% and 10%, (w/w)] were carried out in a reaction kettle. To carry out the homopolymerization reaction, 20 gram of CO was placed in a reaction kettle fitted with a thermometer, condenser and an inlet for the introduction of nitrogen. 10mL of toluene was then added to the kettle and mixed thoroughly with CO. AIBN (0.2 gram) was subsequently added to the mixture for acting as an initiator for the polymerization reaction. Finally, the kettle was placed on a magnetic stirrer and the mixture was maintained at 363 K for 8 hour to prepare the homopolymer. After the fixed time, the reaction mixture was poured into methanol with continuous stirring to terminate the polymerization and precipitate the polymer. For

further purification, the polymers were dissolved in hexane and were repeatedly precipitated by methanol followed by drying under vacuum at 313 K.

For the copolymerization reaction, 20 gram total of CO was taken with 5%, 7.5% or 10% of α-pinene. The copolymerization was similarly carried out in a reaction kettle additionally attached with a dropping funnel to add α-pinene drop wise. The required mass of CO and initiator AIBN (1% by weight with respect to the monomers) was placed in the flask, followed by the drop wise addition of the required mass of α-pinene for 2 hours. The reaction temperature was maintained at 363 K for 48 hour until the polymerisations were complete. The polymers were then purified as reported for the homopolymer. The polymer designations and the composition of the monomers in the copolymers are given in Table 2.4.3.

2.4.2.3 Preparation of bio-additive based lubricating oil formulations

The prepared bio-additives (polymers) were mixed with the two types of base oils (BO1 and BO2) in different percentage ratios (1% to 5%, w/w). The blends were stirred in batches of 200cm^3 at 323 K for 4 hour, at a rotational speed of 300 rpm, to obtain uniform additive dispersion in the lubricants. The blends were then cooled down to room temperature for further study.

2.4.3 Measurements

2.4.3.1 Spectroscopic measurements

For recording the NMR spectra, the selected instrument was a Bruker Avance (Germany) 300 MHz FT-NMR using a 5 mm BBO probe. Here $CDCl_3$ was used as solvent

and tetramethylsilane (TMS) as a reference material. The infrared spectra were recorded on a Shimadzu (Japan) FT-IR 8300 spectrometer, within the wavenumber range of 400 to 4000 cm^{-1} using 0.1 mm KBr cells at room temperature.

2.4.3.2 Thermo-oxidative stability measurements

A thermogravimetric analyzer (Shimadzu TGA-50, Japan) was used to establish the thermo-oxidative stabilities of all the prepared additives. The additives were heated in air using an alumina crucible at a rate of 10 °C per min. Their thermal stability can be measured in terms of percentage of weight loss (PWL) or percentage of residual weight with rise in temperature. The PWL was determined by the equation,

$$PWL = [(M_0 - M_1)/M_0] \times 100 \quad \text{Eq. (1)}$$

where M_0 is the initial mass and M_1 is the remaining mass after the test until constant weight.

2.4.3.3 Determination of average molecular weight

A GPC device (Waters Corporation, USA) was used to establish the average molecular weight (M_w and M_n) and PDI (M_w/M_n) of the prepared additives. The GPC arrangement (polystyrene calibration) was connected with a 2414 refractive index detector, Waters 515 HPLC pump and a 717 plus autosampler. HPLC grade THF was used as an eluent for the instrument at a flow rate of 1.0 mL/min at 30 °C. Table 2.4.4 shows the average molecular weight values as calculated by GPC.

2.4.3.4 Evaluation of pour point (PP)

The pour points of the base oils mixed with different amount of the prepared additives were tested in the temperature range of 0 to −71 °C according to ASTM D97 method on a cloud and pour point tester (Wadegati labequip Pvt., Ltd., India).

2.4.3.5 Evaluation of viscosity index (VI)

The alteration of kinematic viscosity (KV) of oil with the variation of temperature is denoted by an arbitrary dimensionless number called viscosity index (VI). A higher value of VI signifies a relatively small change in viscosity with the temperature variation.

The VI was evaluated according to the ASTM D2270 method for the two base oils blended with different percentages of the additive at 313 K and 373 K (ASTM 2004). The effectiveness of an additive as VII is assessed by the increase in the VI value of the base oils after addition of the additive. The KV was determined by the equation,

$$KV = (Kt - L/t)\,\rho \qquad \text{Eq. (2)}$$

where K and L are viscometric constants; t is the time of flow of the lube oil blended with different mass fraction of the additive to pass through the two calibrated marks in the Ubbelohde viscometer and ρ is density of the additive doped lube oil.[15]

The densities of the additive doped oils were determined with the help of a DMA 4500 M vibrating-tube density meter (Anton paar, Austria) and the time of flow of the oils was recorded with a digital stopwatch. All the measurements per batch were made in duplicate. The VI value was determined from the following standard empirical equation,

$$VI = 3.63(60 - 10^{n}) \qquad \text{Eq. (3)}$$

where *n* is a constant depending upon the temperature range chosen for the oil. The value of *n* was calculated by the equation,

$n = (\ln \nu_1 - \ln k)/\ln \nu_2$ Eq. (4)

where ν_1 and ν_2 are the kinematic viscosities of the oil blended with the additive at lower and higher temperature respectively. The value of k is independent of the nature of the oil and is a function of temperature alone. For the given temperature range, the value of k was found to be 2.715.[16]

2.4.3.6 Photo micrograph and wax modification

The photomicrographs presenting wax crystallization behaviour of the base oils mixed with different ratios of the prepared additive were recorded in a Banbros polarizing microscope (BPL-400B, India). The temperature was set at 273 K and it was suitably controlled on the microscope slide by an attached cooling thermostat. The magnification used here was 200X.

2.4.3.7 Biodegradability test

Biodegradation can be defined as the mineralisation or breakdown of an organic matter due to microbial activity, leading to a significant change in its chemical structure. If complete biodegradation takes place under aerobic conditions the material will be converted to carbon dioxide and water, while under anaerobic conditions the organic carbon of the material will be converted to biogas. In both cases, the organic carbon is also partly converted to new biomass.

Out of the several techniques of examining the chemicals for biodegradation, the soil burial degradation test as per ISO 846:1997 and the disc diffusion test against fungal pathogen were chosen here.[17,18] PWL [Eq. (1)] of the additives was analysed to examine the magnitude of degradation in the burial test. The shift in the IR frequency of the ester carbonyls after the biodegradability test along with the change in their molecular mass was also a parameter to judge the degradation of the additives.

2.4.3.7.1 Soil burial degradation test (SBD test)

The soil used for this test had been obtained from the campus of North Bengal University (West Bengal, India) with a measured value of pH 7.2 and moisture content of 26%. The soil was first taken in a humidity chamber, set at 303 K, to adjust the relative humidity to around 60%. Separate polymeric films were produced from all the additives by taking 2 gram of the additives in each case.[19] The films were then buried in the soil (containing the microorganisms) in a bacteriological incubator (Sigma Scientific Instruments Pvt., Ltd., India). After every 15 days, the buried additive films were taken out for analysis and the process was repeated for a period of 90 days with a different film used for each time period. The recovered polymeric films were cleaned with chloroform, filtered with Whatman grade 41 filtration paper and then dried in a vacuum oven at 323 K. They were again purified by dissolution in hexane and reprecipitation with methanol followed by drying under vacuum at 323 K to constant weight. For each of the films, the weights after drying were recorded to verify the percentage of weight loss.

2.4.3.7.2 Disc diffusion (DD) test

The disc diffusion test includes the arrangement of culture media for the fungal strains and assessing the biodegradation of the additives against fungal pathogens. Here the biodegradation was tested for the fungal pathogen, *Alternaria alternate* (AA). For creating the culture media, dextrose, agar powder and potato extract were mixed in a ratio of 1:1:10 by weight. For this test, 2 gram of the synthesised additive was taken in a sterilized Petri dish and inoculated by spraying the fungal pathogen. To keep away from any further contamination, the sterilized Petri dish was sealed by wax and incubated at 310 K in a bacteriological incubator. The whole procedure was implemented for all the additives separately with the fungal pathogen. During incubation, the spores (colonies) emerging as black spots were observed to grow suggesting the fungal growth on the additives. After a stretch of 30 days, the additives were recovered from the culture and rinsed with chloroform, filtered with Whatman grade 41 filtration paper and dried in a vacuum oven at 323 K. PWL was computed for all the additives and their molecular weights were calculated by GPC analysis.

2.4.4 Results and discussion

2.4.4.1 Spectroscopic data analysis

FT-IR Spectroscopy: The FT-IR spectra of HCO (P-1, homopolymer of castor oil) showed signal for the stretching vibration of ester carbonyl group (C=O) at 1741 cm^{-1} while the peak (broad) for ester C–O stretching vibration appeared at 1174 cm^{-1}. Peaks in the region of 1460 cm^{-1}, 1375 cm^{-1} and 724 cm^{-1} were for the bending vibrations of the C–H bonds. The intense absorptions at 2855 cm^{-1} and at 2927 cm^{-1} are attributed to the stretching vibrations of the paraffinic C–H bonds. The broad IR transmission at 3438 cm^{-1} indicated the presence of O–H stretching of the alcoholic moiety of ricinoleic acid

present in castor oil (Fig. 2.4.2). Additives P-2, P-3 and P-4 have almost similar IR peaks (Figs. 2.4.3, 2.4.4 and 2.4.5). In their spectra, the peaks at 1746, 1744 and at 1745 cm^{-1} pointed out the existence of ester carbonyl groups. The ester C–O proved their presence by vibrating (stretching vibrations) at 1168, 1172 and 1168 cm^{-1} respectively. Their IR spectrum also had characteristic peaks at 721 to 724 cm^{-1}, 1373 to 1375 cm^{-1} and 1451 to 1461 cm^{-1} representing the bending vibrations of the C–H bonds for the methylene and methyl groups of castor oil and α-pinene. The observed transmissions at 2852 to 2855 cm^{-1} and 2919 to 2926 cm^{-1} were caused by the stretching of C–H bonds. The characteristics O–H stretching peaks were present in all the additives at 3414, 3406 and at 3417 cm^{-1} respectively. The lack of any peaks in the range of 1600 cm^{-1} to 1680 cm^{-1} pointed out the nonexistence of any olefinic carbon in the additives and therefore the formation of the desired product.

^{1}H-NMR: The proton NMR spectroscopy showed multiple peaks in the spectra of the additives. HCO showed signal for the methyl protons at δ 0.82 ppm while the signals in the range of δ 1.24 to 2.16 ppm appeared for the methylene protons of alkyl groups. The presence of $–OCOCH_2–$ moiety in castor oil is showed by the chemical shift between δ 2.25 and 2.27 ppm while the hydrogens of the –OH group of ricinoleic acid appeared as broad peak centered at δ 3.57 ppm. The signals in the spectra between δ 4.09 and 4.25 ppm appeared due to the protons of $–COOCH_2$ groups of the triglyceride of castor oil. Any useful proton peaks were found to be missing between δ 5.5 and 6.5 ppm signifying complete utilisation of olefinic groups in the polymerisation process (Fig. 2.4.6). The other copolymer (P-2 to P-4) showed nearly similar chemical shifts between δ 0.81 and 0.82 ppm for the methyl protons. The peaks between δ 1.24 and 2.19 ppm appeared because of the methylene protons of castor oil and α-pinene, while the signals between δ 2.22 and 2.69 ppm is attributed to the protons of $–OCOCH_2–$ groups. The peaks

between δ 3.54 to 3.66 ppm are credited to the –OH group of castor oil while the protons of $-COOCH_2$ groups showed signals in the range of δ 4.04 to 4.26 ppm. Also the nonappearance of any signals between δ 5.5 and 6.5 ppm in the proton NMR spectra point towards the absence of sp^2 carbons in the copolymers (Figs. 2.4.7, 2.4.8 and 2.4.9).

^{13}C-NMR: All the sp^3 ($-CH_3$ and $-CH_2$) carbon atoms of the alkyl chain of castor oil, present in HCO, appeared between δ 12 and 36 ppm in the ^{13}C NMR spectra. The $-COOCH_2$ groups in the triglyceride backbone of castor oil indicated their presence by the signals between δ 61 and 68 ppm. Peak appearing at δ 70 ppm indicated the carbon joined to the –OH group of the ricinoleic acid present in castor oil and the signals between δ 172 and 173 ppm is credited to the carbonyl carbon of the ester group. HCO displayed no peaks between δ 120 and 150 ppm, signifying the successful conversion of olefinic carbons to saturated carbons during polymerisation (Fig. 2.4.10). The other polymers (P-2, P-3 and P-4) displayed similar ^{13}C spectra with observed transmissions between δ 14 and 37 ppm indicating the sp^3 carbons of castor oil and α-pinene. The signals between δ 62 to 69 ppm are attributed to the presence of $-COOCH_2$ groups of the triglyceride moiety. The peaks ranging from δ 70 to 72 ppm appeared because of the carbon joined to the –OH group in castor oil while the carbonyl carbons showed their presence between δ 170 and 178 ppm. Also, no signals were present between δ 120 and 150 ppm in any of the copolymers (Figs. 2.4.11, 2.4.12 and 2.4.13).

2.4.4.2 Thermogravimetric analysis (TGA)

Fig. 2.4.16 presents a comparative data of the thermogravimetric analysis of the synthesised additives. After thermal degradation, at 300 ^{o}C, the percentages of residual weight of the additives P-1, P-2, P-3 and P-4 were found to be 50.35, 79.53, 75.19 and

73.23 respectively. At 400 ^{o}C the amount (percentages of residual weight) left were 2.28, 52.65, 46.36 and 43.84 respectively. The results showed that the copolymers were better in thermo-oxidative stability than the homopolymers. Moreover, as suggested by the percentage of residual weight values, the thermal strength of copolymers increased with decreasing α-pinene fraction in the additives. Also, the thermal degradation of additive P-2 was found to be the least. This increased thermal stability of the additive P-2 is probably due to its comparatively narrower molecular weight distribution (as suggested by the PDI value) and the highest molecular weight among the additives.[20]

2.4.4.3 Analysis of pour point data

The pour points of the additive-doped lube oils were tested by mixing the additives at different fractions (1% to 5%, w/w) with the base oils (BO1 and BO2) and the investigational results are plotted in Figs. 2.4.17 and 2.4.18. It is clearly noticed that the effectiveness of the additives as PPD gradually became better with increase in their concentration in the base oils. Moreover, with the increment of α-pinene fraction in the additive their effectiveness as PPD gradually decreased. PPDs typically have no impact on the crystallization temperature. Though, the improvement in the PPD properties of an additive is as a consequence of disruption of the rigid network of wax crystals that are formed at lower temperatures from the dissolved waxy hydrocarbons present in mineral oils. The size and growth of wax crystals can be suitably controlled by PPDs and thereby the ability of these crystals to flocculate and interlock among themselves.[21]

These depressants control the crystal growth either by adsorption on the precipitating wax or by cocrystalization. PPDs typically have a paraffinic part that resembles the wax structure and, hence, cocrystallizes with the oil's wax forming

components and becomes associated with them while the polar section present in the PPDs confines their extent of cocrystallization.[22] Improved wax solubility and nucleation are also among the other theories suggested for the mechanism of action of PPDs.[23] The PPD property of the additive P-1 was better here as compared to the other additives with different concentrations of α-pinene. The reason for this is possibly the better interaction of additive P-1with the wax crystals when compare to the others. The extent of interaction varies with the polarity of additive molecules and a more polar additive can form stronger H-bond with the polar groups of resin and asphaltene present in the base oil.[24] The high percentage of ricinoleic acid (with polar hydroxyl group) in castor oil (Fig. 2.4.1) makes them highly polar and the incorporation of α-pinene in the castor oil moiety diminishes the polarity of the overall additive molecule. This reduction in their polarity decreases their effectiveness to act as an efficient PPD.

2.4.4.4 Analysis of viscosity index data

The result, as presented in Fig. 2.4.19, explains that the VI of the base stocks mixed with the additives were significantly superior compared to the base stocks lacking the additives. The investigation also revealed that irrespective of the nature of the base stock and the additive, the VI improved with enhancement in the additive concentration. All the additives (P-1 to P-4) showed excellent results but the incorporation of α-pinene to CO enhanced the VI to a much greater extent. Among all the additives, at a 5 wt % of additive concentration, additive P-4 showed the highest increase of VI for both the base stocks (VI value 167 for BO1 and 174 for BO2). At the same concentration, additive P-1 (HCO) produced a VI of only 144 and 150 for BO1 and BO2 respectively. The VI values as plotted in Fig. 2.4.19, increased in the order P-1 < P-2

< P-3 < P-4. The ability to act as a viscosity index improver, by any polymer, is governed by its chain topology, temperature dependent solubility, molecular weight and structure of polymeric macromolecules.[25] These factors decide the hydrodynamic volume of the haphazardly curled polymer chain which in turn compensates the reduction of the viscosity of the base oil with increasing temperature. It is believed that in the base oil, the polymer molecules remain in a coiled shape. With increasing temperature, the polymer coils expands ensuing an enhancement in polymer chain entanglements. Besides, with increase in polymer percentage, the interaction between the base oil and these macromolecules also increases ensuring a greater thickening and a higher VI for the oil.[26] The VI obtained for the copolymers here are higher than P-1 and the results may be attributed to their greater molecular weight and narrower molecular weight distributions. Polymers with hyper-branched structure and with the compact chain arrangement have a reduced hydrodynamic volume compared to the polymers of linear chain topology of similar molecular weight. Additionally, as a result of their restricted hydrodynamic volume, these hyper-branched polymers hinder the spreading out of polymer coil dimension resulting in reduced chain entanglements among themselves.[27] Hence, additive P-4 with high molecular weight and the most linear chain topology produced a greater thickening of the oil and in doing so generated the highest VI.

2.4.4.5 Analysis of photo micrographic image

The study of photo micrographic image of the lube oil helps to understand the effect of additives on their pour point values. The photomicrographs depicted in Fig. 2.4.20 gave a picture of the variation of wax morphology according to the nature of additives added. Fig. 2.4.20a, which represents the pure base oil, showed large cyclic

and needle shaped wax crystals of approximate size of 100 μm. The base oil when blended with 4% (w/w) of the additives, showed a substantial reduction in the size of wax crystals. The large crystals were converted into numerous finely dispersed crystals. A higher wax alteration was noticed for the additive P-1(Fig. 2.4.20b) with most finely dispersed wax crystals while the additive P-4 (Fig. 2.4.20e) showed the least wax modification. Study of the photomicrographs thus revealed that additive P-1 acted as a better PPD than the other additives. So, the wax modification results, as illustrated by the photomicrographs are in good agreement with the flow parameter (pour point) of the additives determined by the ASTM method.

2.4.4.6 Analysis of biodegradability test

The additives here are all synthesised from natural monomer units and are likely to show significant amount of biodegradability. The biodegradability test results procured by analysing the disc diffusion test and the soil burial test methods are presented in Table 2.4.5 and Fig. 2.4.21 respectively and the results reflected plenteous bio-assimilation for the additives.

In the SBD test, the breakdown of all the additives by the soil microbes escalated with the increasing number of days. After 90 days, the additive P-1 exhibited the highest degradation among the other additives with a weight loss of 27.6%. After the same time period, additive P-4 exhibited a weight loss of 19.5% which is least amid all the additives.

The analysis of the DD test also displayed similar trend against the fungal pathogen. The bio-assimilation of additive P-1 was the highest in this test as well with 30.3 % weight loss after a span of 30 days. The PWL of the other additives (P-2, P-3 and

P-4) were 26.7, 22.9 and 19.7 respectively after the same stretch of 30 days. GPC of the additives after the DD test was also conducted and the numbers were compared with the respective additives before biodegradation (Table 2.4.5). The figures reflected sizeable change in the M_n and M_w of the additives and thus revealed the biodegradability of the prepared additives.[28]

The FT-IR spectra of the additives, before and after the DD test were also studied to identify any shift in their IR peaks (Figs. 2.4.14 and 2.4.15). The signal of the ester carbonyl group at 1741 cm^{-1}, for the additive P-1, shifted noticeably to 1728 cm^{-1} with a decrease in the peak height and intensity after the test. IR transmissions of the additive at 724, 854, 1174, 1243, 1375, 1460 and 3438 cm^{-1} has also shifted markedly after the DD test. Similar shift in the IR signals were noticed for the other additives as well. This shift in the IR peaks is possibly due to the scission of the polymer units after biodegradation.[29] These variations in the IR peaks of the additives, the change in their weight-average molecular weight (M_w) and number-average molecular weight (M_n) along with their PWL confirmed the biocompatible property of the prepared additives.

2.4.5 Conclusions

In this work, thorough analyses of the synthesised polymers were carried out to assess their performance as a multifunctional additive. The results pointed out that mixing of these additives to the base oil improved their lubricant property greatly. A comprehensive study of the additives showed that the copolymers were superior as VII. The most significant viscosity increment was displayed by the additive P-4 while the additive blend P-1 exhibited superior performance as PPD for the lube oils under examination. The application of copolymer always yielded a significant increase in

thermal stability and the additive P-2 had the best performance. Furthermore, the study illuminated that all the additives are also environmentally benign. Therefore, the prepared bio-additives may be used for designing green bio-lubricant formulations for lube oil to satisfy the mounting environmental and performance concerns of modern lubricants.

2.4.6 References

References are given in BIBLIOGRAPHY under Chapter-IV of Part-II (Page No. 220-223).

2.4.7 Tables and figures

Table 2.4.1: Physical properties of base oils

Properties	**Method**	**BO1**	**BO2**
Viscosity at 40 °C in cSt	ASTM D445	7.229	23.472
Viscosity at 100 °C in cSt	ASTM D445	1.874	3.938
Viscosity Index	ASTM D2270	81	86
Pour Point, °C	ASTM D97	-3	-6
Density ($g.cm^{-3}$) at 40 °C	ASTM D4052	0.83689	0.85514

Table 2.4.2: Fatty acid composition of castor oil

Fatty acid	***Average % composition***
Palmitic C16:0	1.7
Stearic C18:0	1.9
Oleic C18:1	5.3
Linoleic C18:2	7.0
Linolenic C18:3	1.5
Ricinoleic C18:1:OH	82.4

Table 2.4.3: Percentage composition and designation of the polymers

Polymers	***% of monomers in the polymers***		***Solvent, Initiator***
	Castor oil	***α-pinene***	
P-1	100	0	Toluene, AIBN
P-2	95	5	Toluene, AIBN
P-3	92.5	7.5	Toluene, AIBN
P-4	90	10	Toluene, AIBN

P-1: Homopolymer of castor oil, P-2: Copolymer of castor oil + 5% α-pinene, P-3: Copolymer of castor oil + 7.5% α-pinene, P-4: Copolymer of castor oil + 10% α-pinene.

Table 2.4.4: Average molecular weight of polymers determined by GPC

Polymers	***Average molecular weights***		
	M_w	M_n	***PDI***
P-1	17882	11247	1.59
P-2	30214	21428	1.41
P-3	29636	21952	1.35
P-4	28574	23421	1.22

Table 2.4.5: Result of biodegradability test by DD method and comparative average molecular weight values determined by GPC

Polymers	***Incubation period (days)***	***Pathogen***	***PWL***	***Molecular weight***			
				Before biodegradation		***After biodegradation***	
				M_w	M_n	M_w	M_n
P-1	30	AA	30.3	17882	11247	15978	10902
P-2	30	AA	26.7	30214	21428	27228	20267
P-3	30	AA	22.9	29636	21952	27134	20873
P-4	30	AA	19.7	28574	23421	26965	22321

Figure 2.4.1: Triester of glycerol and ricinoleic acid (structure of the major component of castor oil)

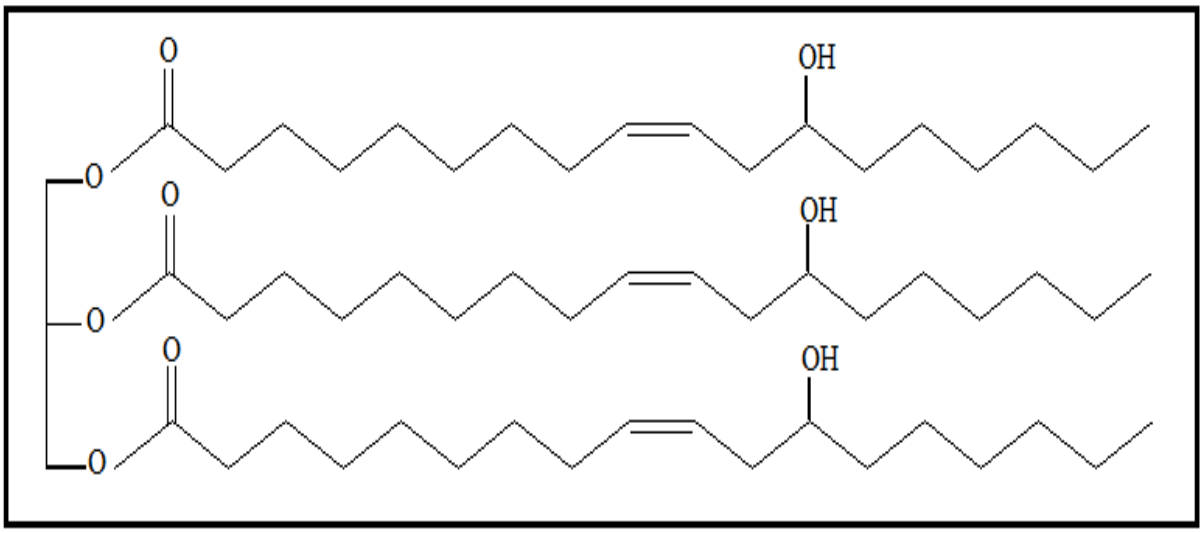

Figure 2.4.2: FT-IR spectra of homopolymer of CO (P-1)

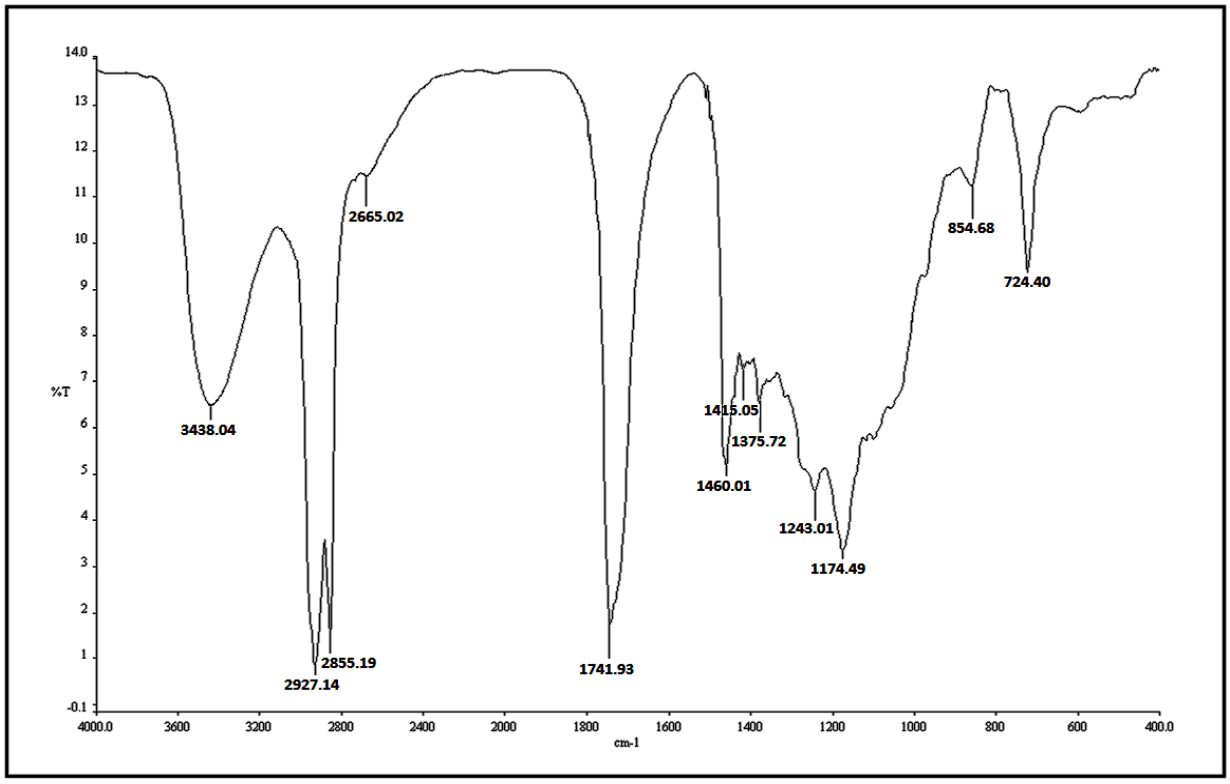

Figure 2.4.3: FT-IR spectra of copolymer of CO with 5% α-pinene (P-2)

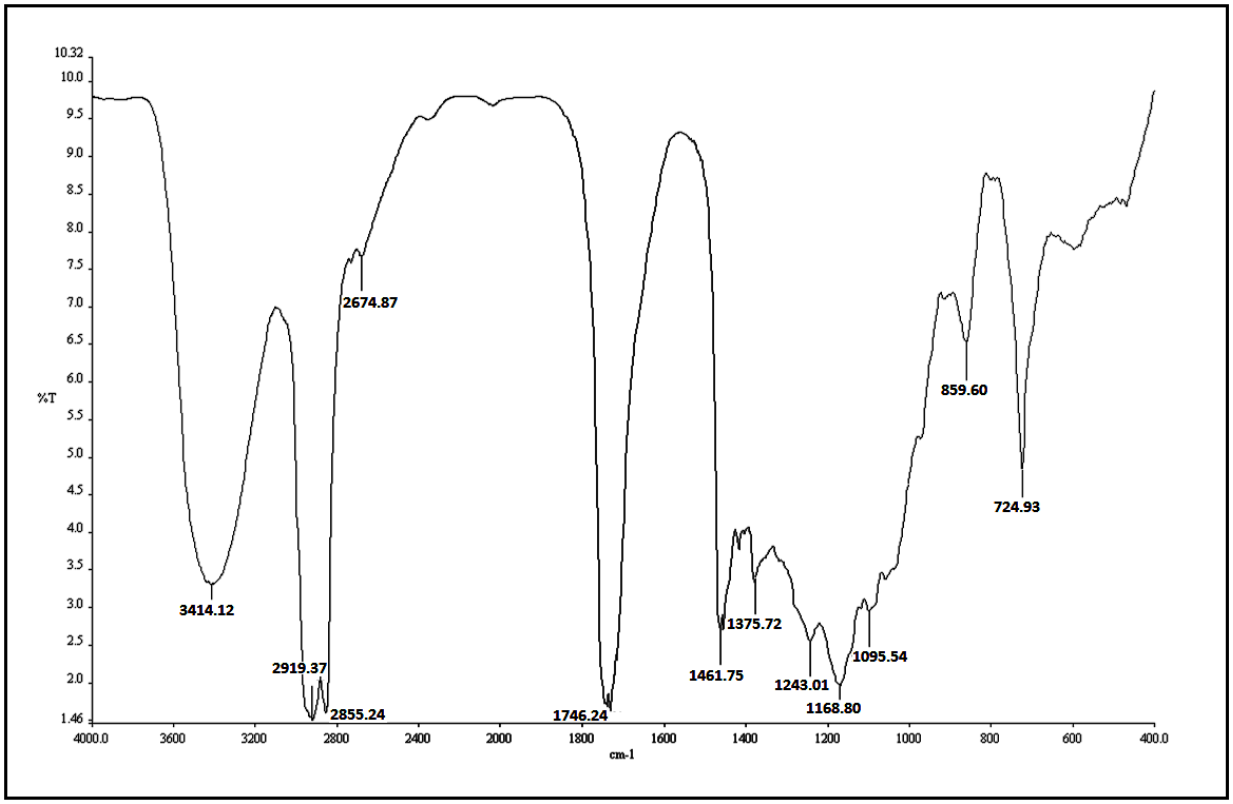

Figure 2.4.4: FT-IR spectra of copolymer of CO with 7.5% α-pinene (P-3)

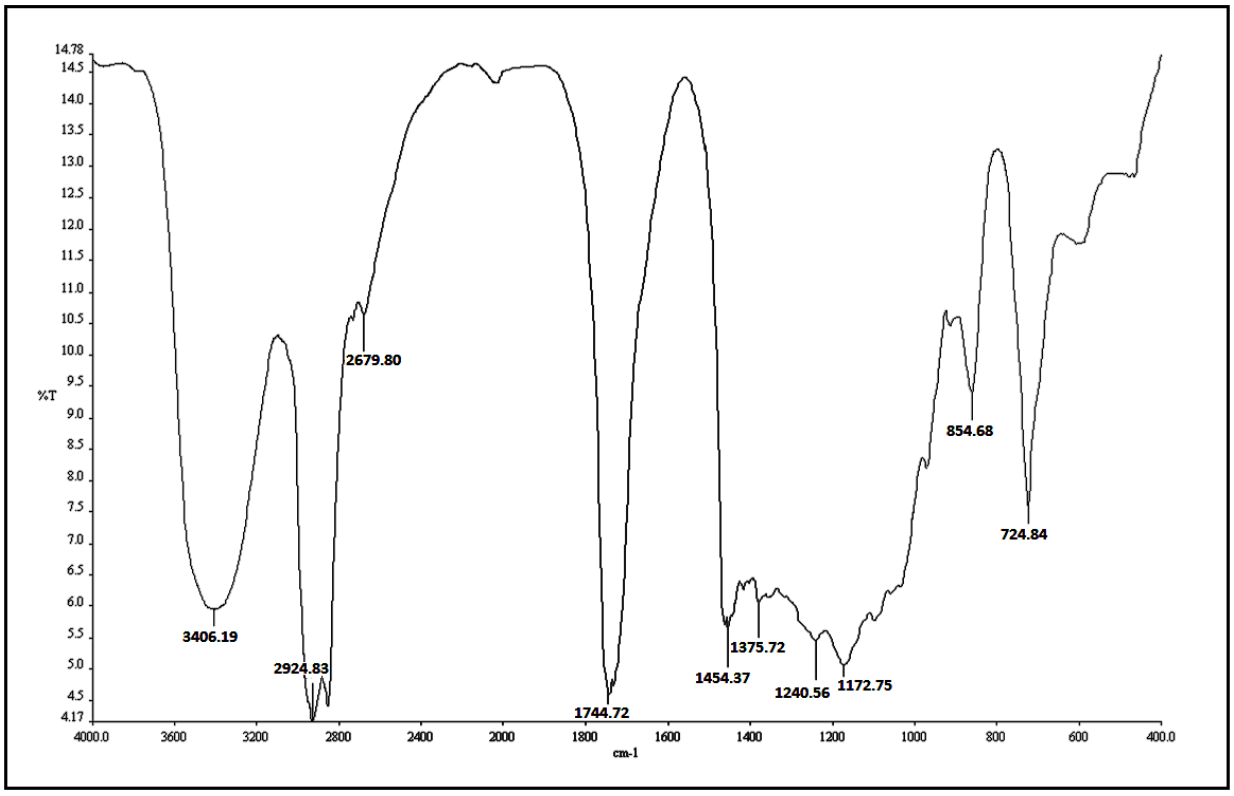

Figure 2.4.5: FT-IR spectra of copolymer of CO with 10% α-pinene (P-4)

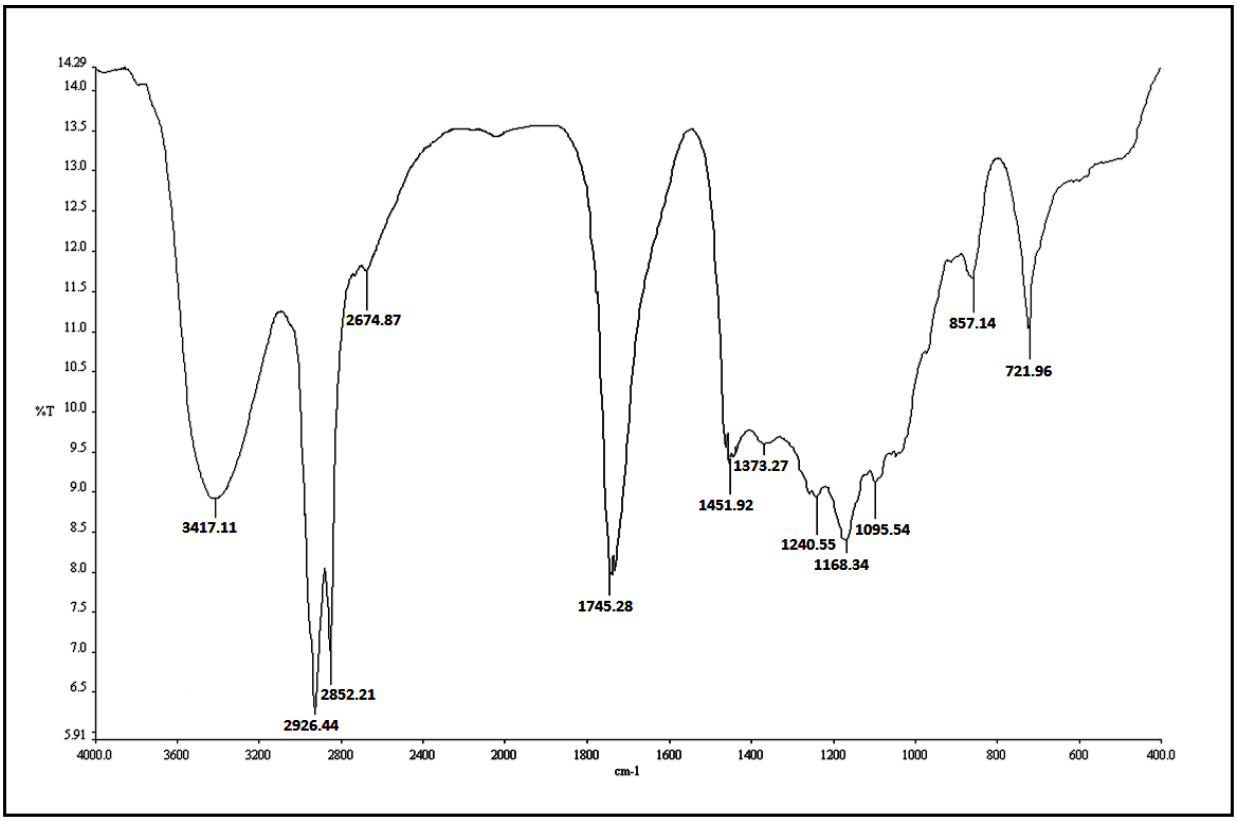

Figure 2.4.6: ^{1}H-NMR spectra of homopolymer of CO (P-1)

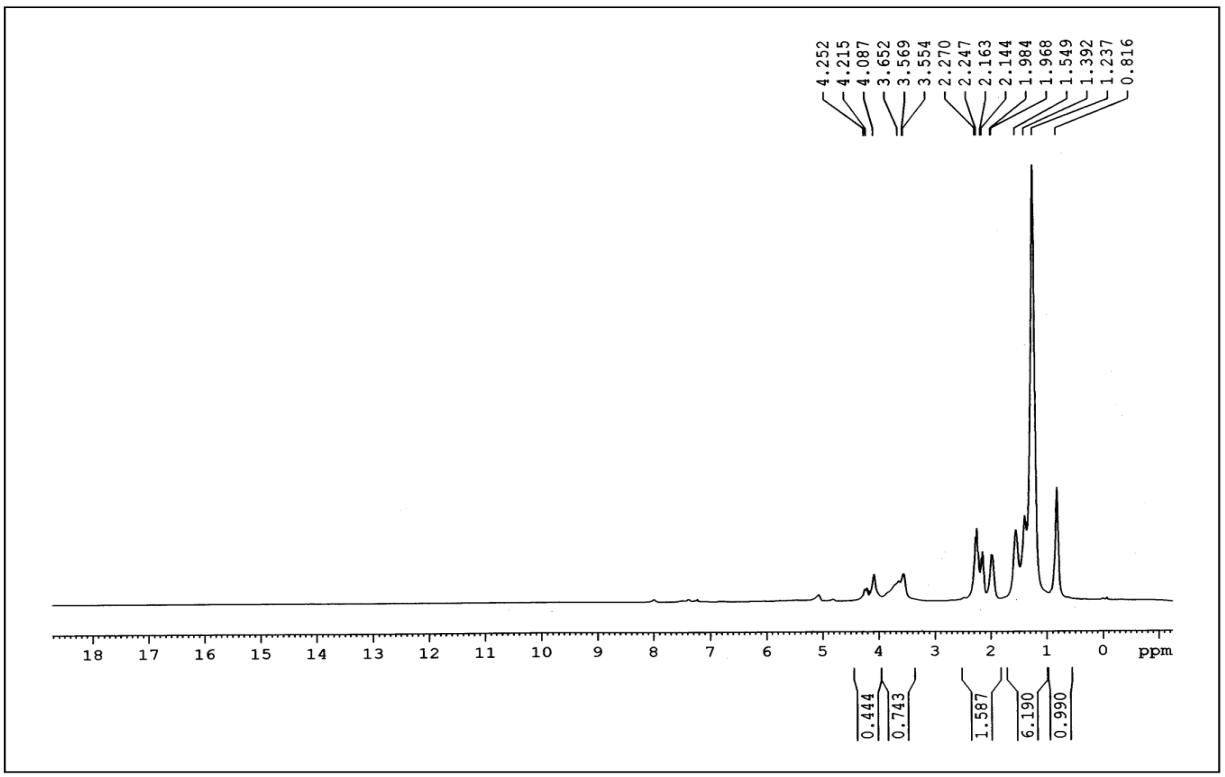

Figure 2.4.7: ^{1}H-NMR spectra of copolymer of CO with 5% α-pinene (P-2)

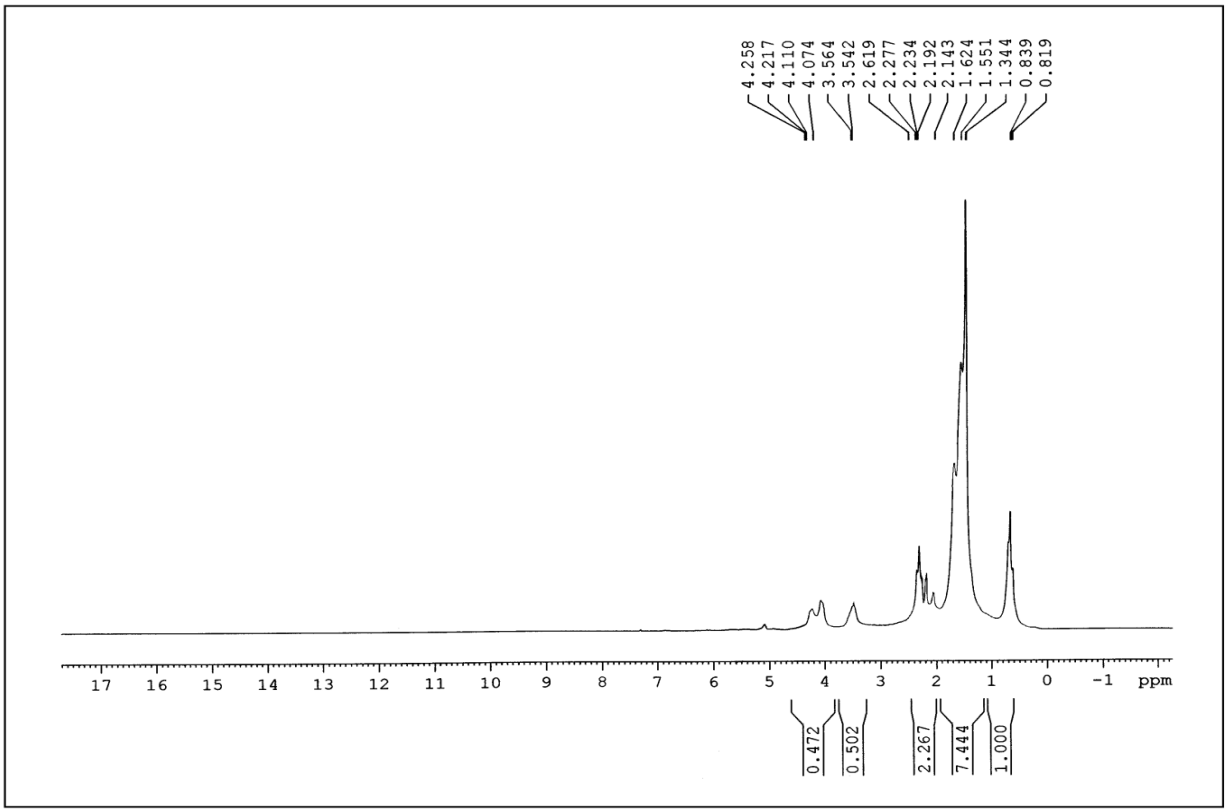

Figure 2.4.8: ^{1}H-NMR spectra of copolymer of CO with 7.5% α-pinene (P-3)

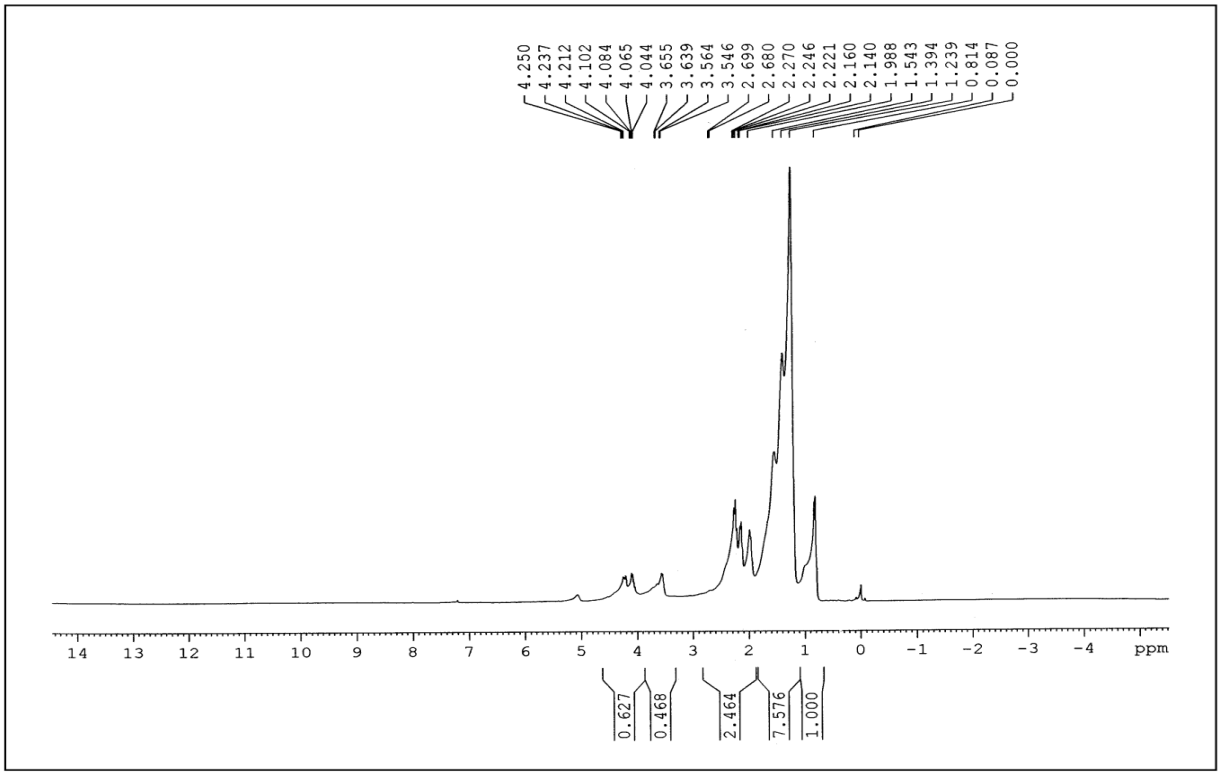

Figure 2.4.9: ^{1}H-NMR spectra of copolymer of CO with 10% α-pinene (P-4)

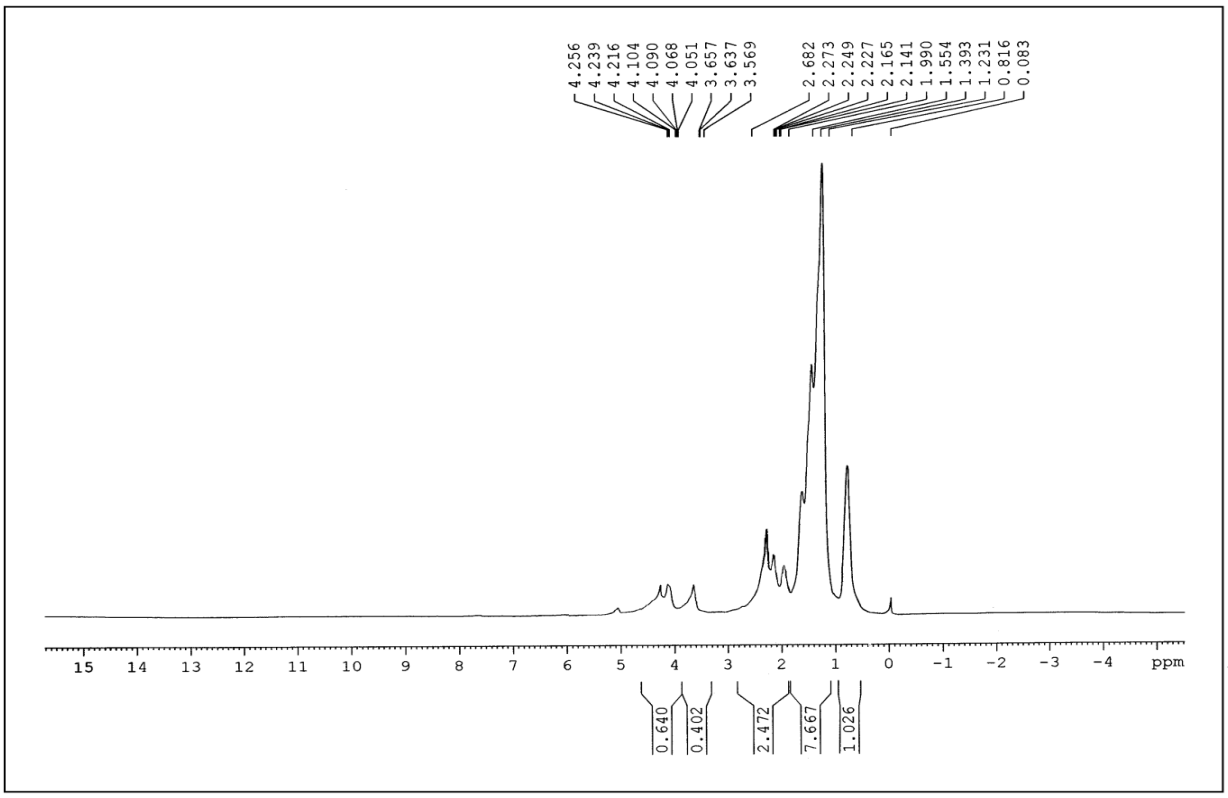

Figure 2.4.10: ^{13}C-NMR spectra of homopolymer of CO (P-1)

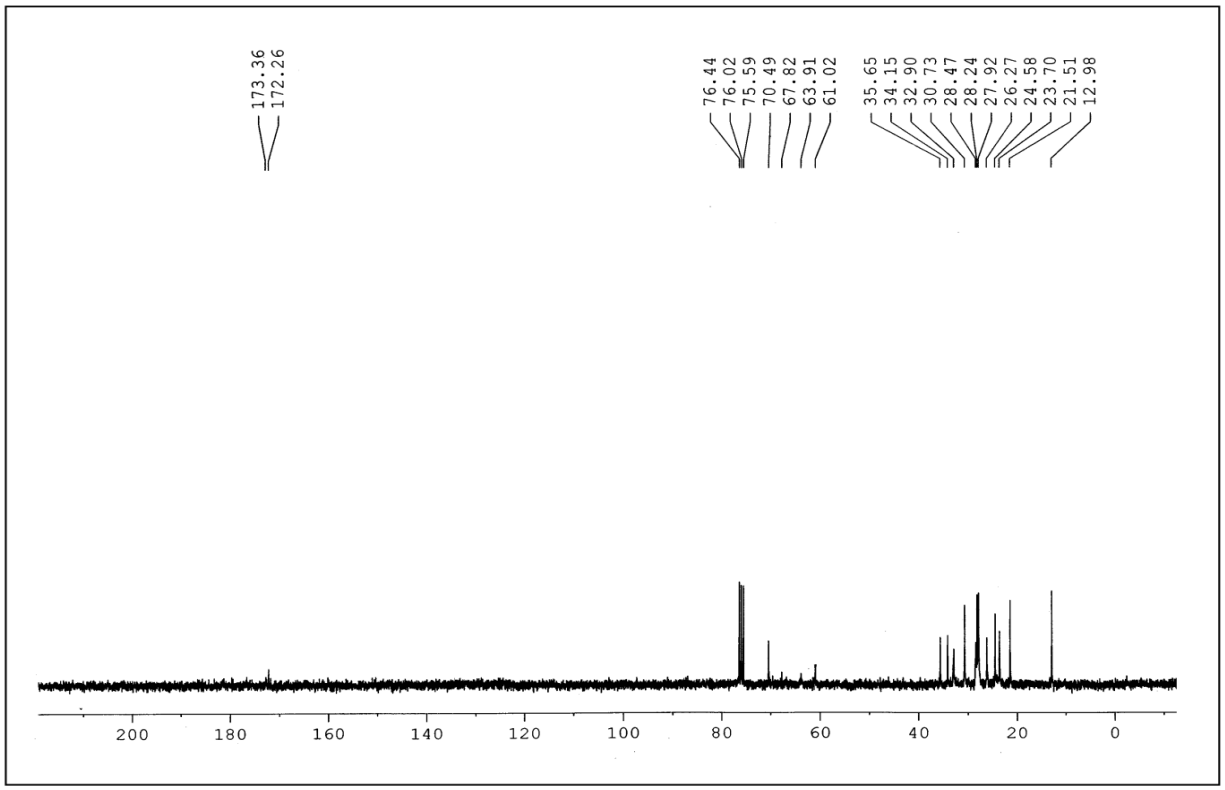

Figure 2.4.11: ^{13}C-NMR spectra of copolymer of CO with 5% α-pinene (P-2)

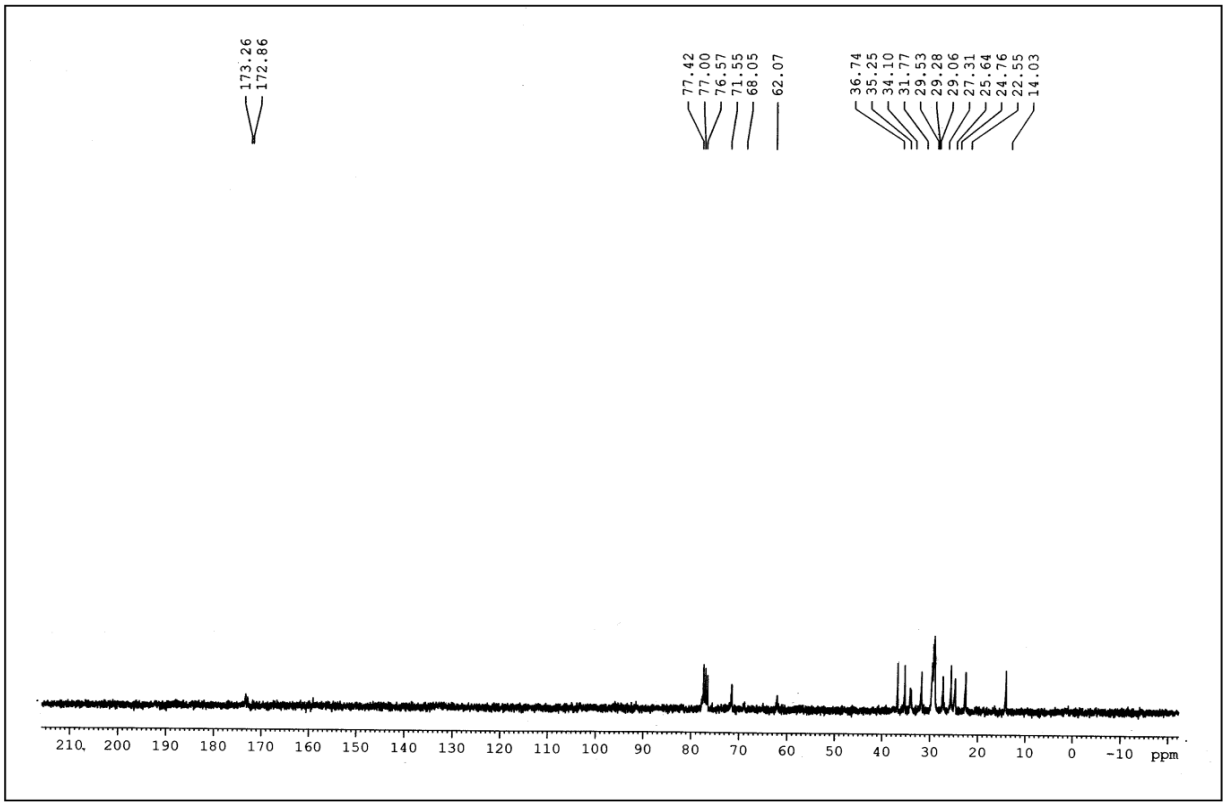

Figure 2.4.12: ^{13}C-NMR spectra of copolymer of CO with 7.5% α-pinene (P-3)

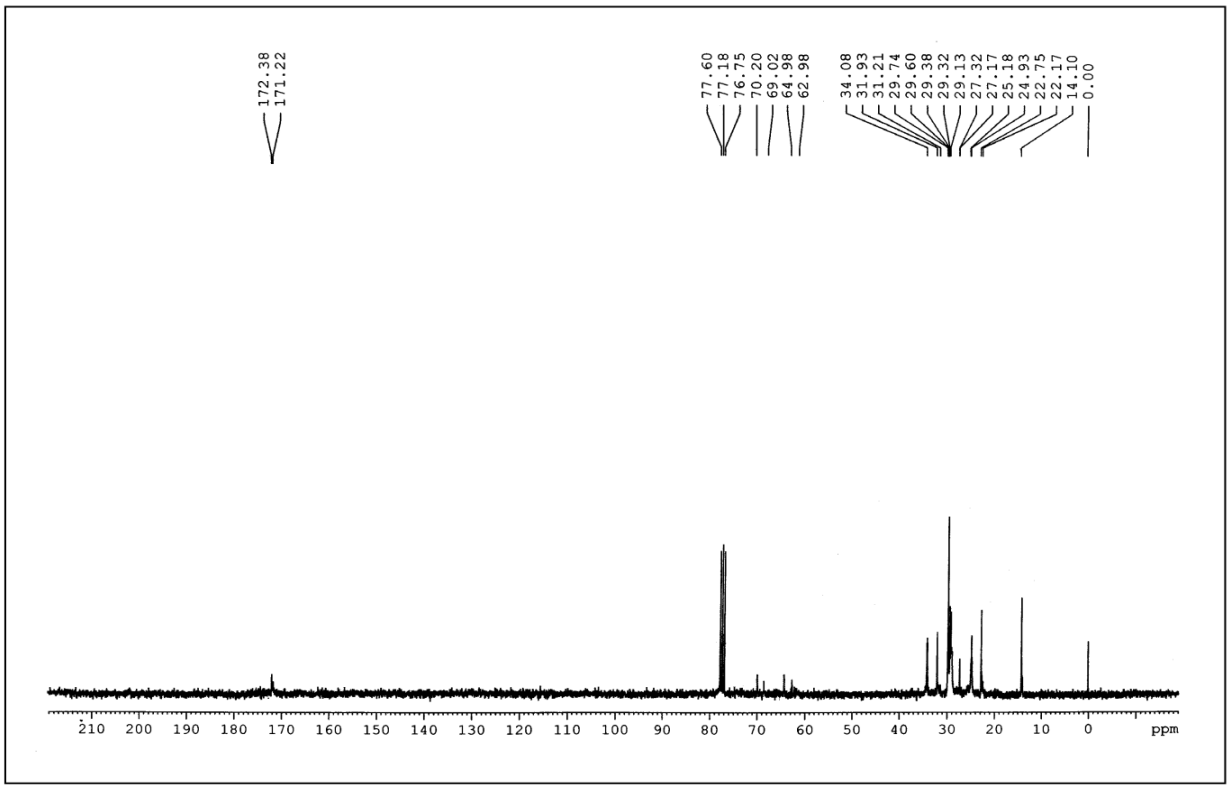

Figure 2.4.13: ^{13}C-NMR spectra of copolymer of CO with 10% α-pinene (P-4)

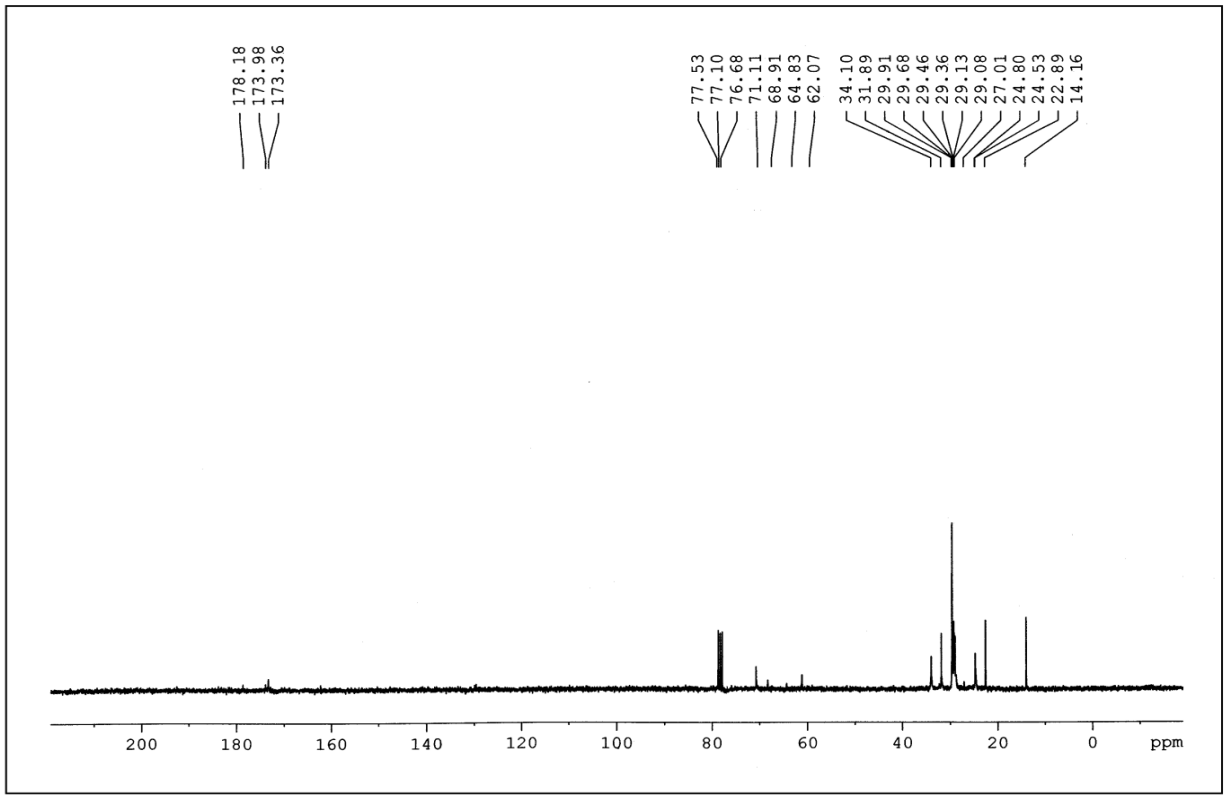

Figure 2.4.14: FT-IR spectra of homopolymer P-1 after biodegradation

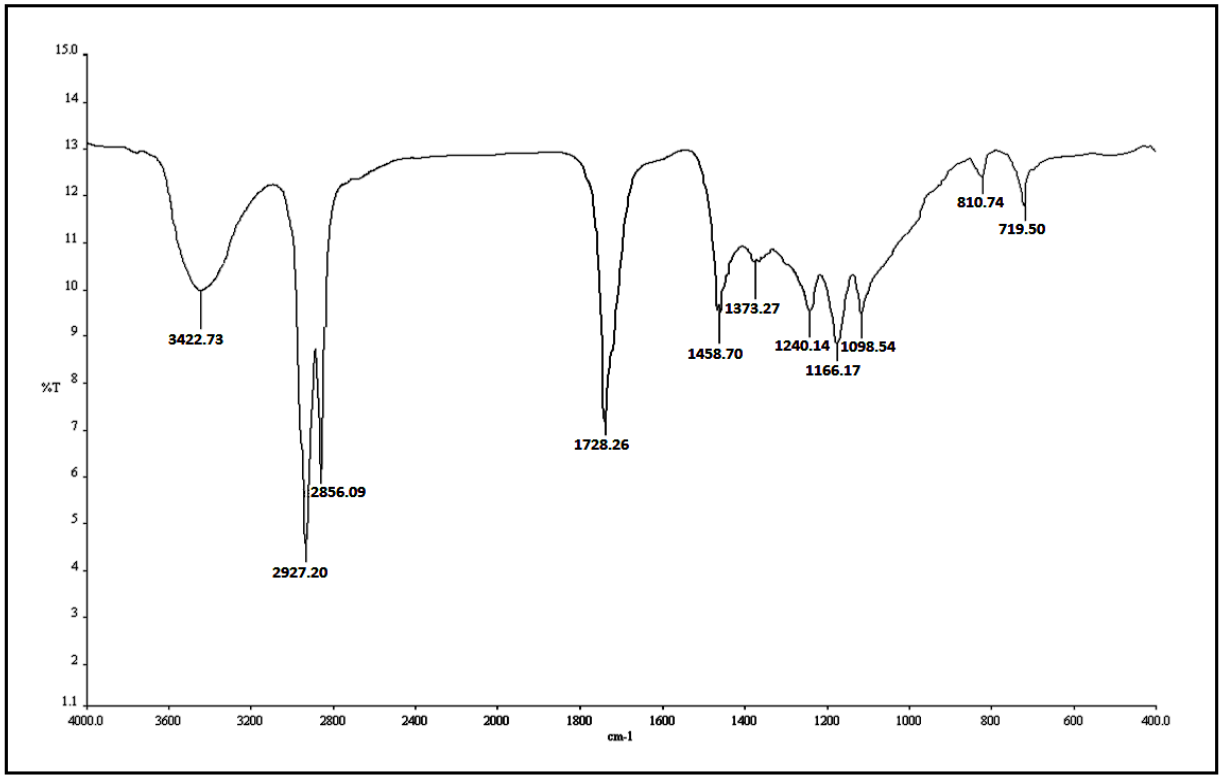

Figure 2.4.15: FT-IR spectra of copolymer P-4 after biodegradation

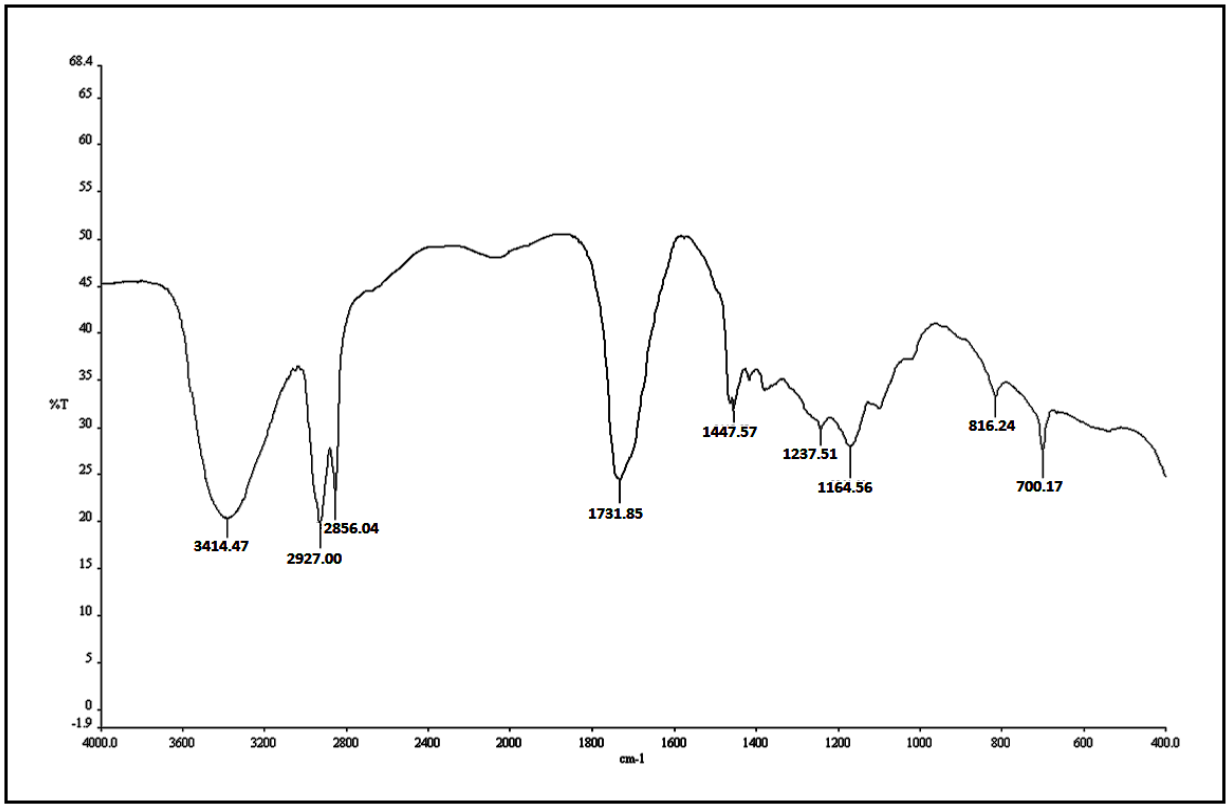

Figure 2.4.16: TGA results of the polymers

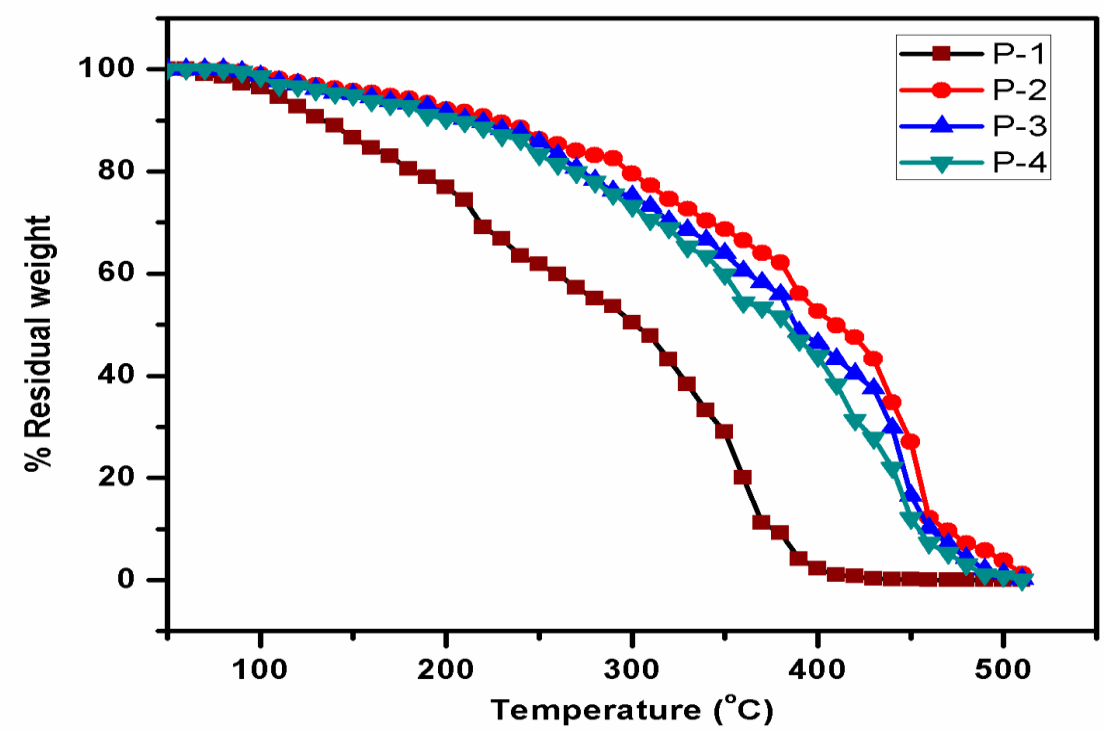

Figure 2.4.17: Pour point variation of the base oil (BO1) blended with additives at different concentrations

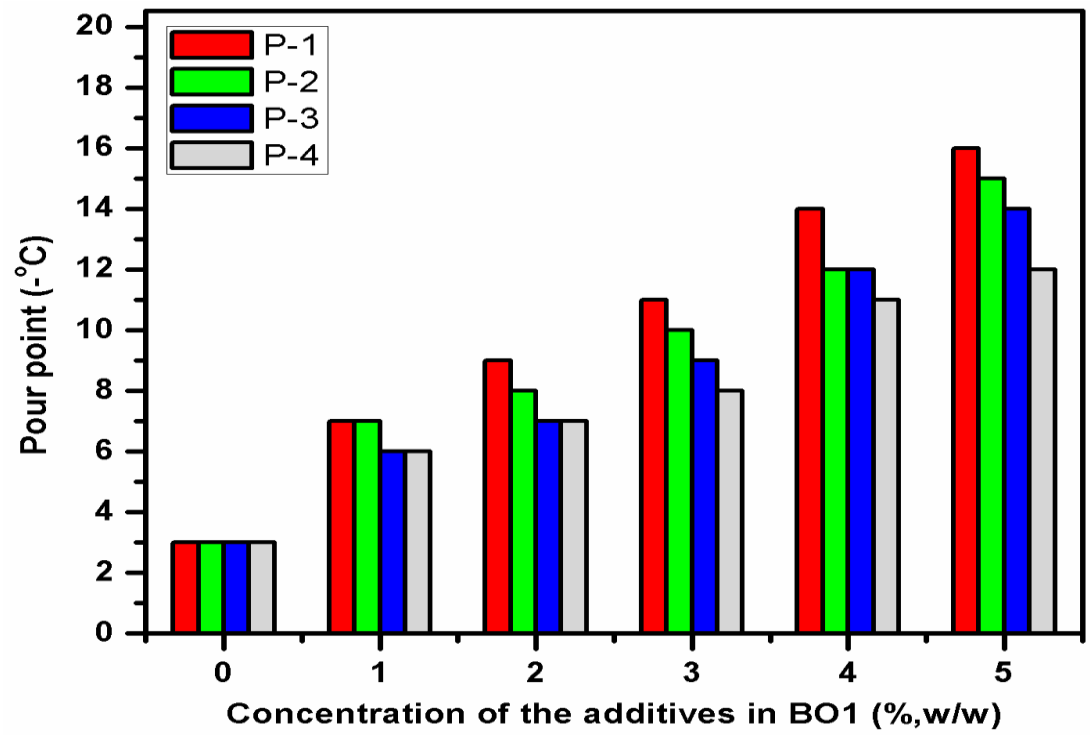

Figure 2.4.18: Pour point variation of the base oil (BO2) blended with additives at different concentrations

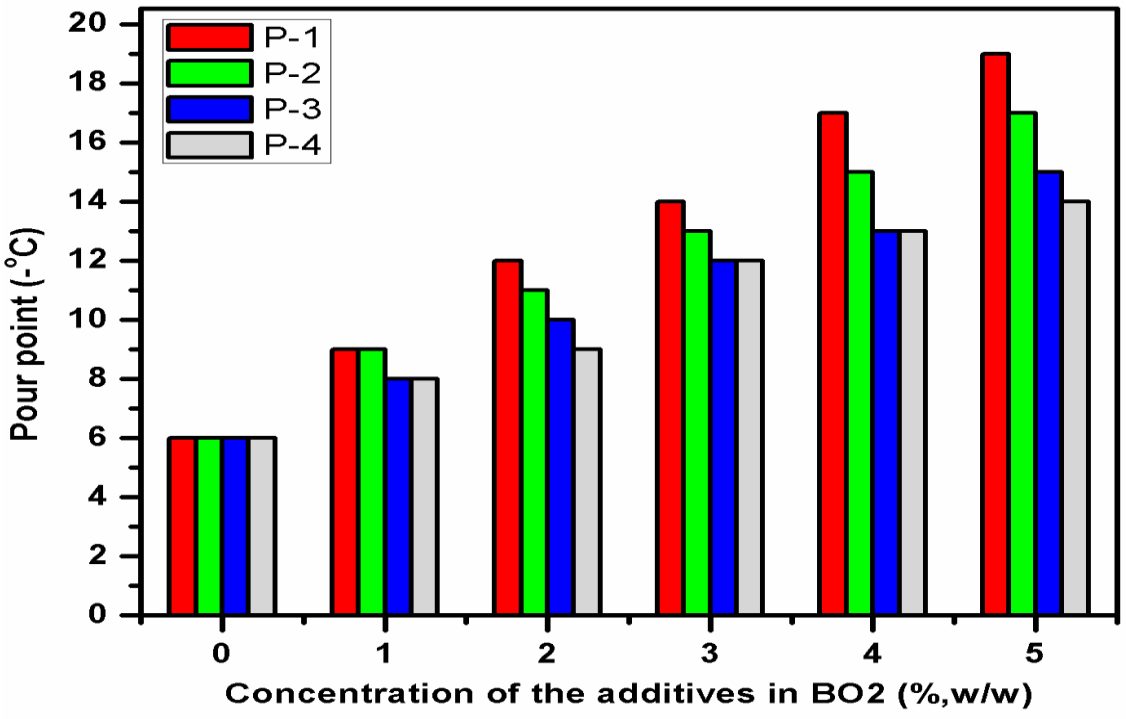

Figure 2.4.19: Viscosity index variation of the base oils (BO1 and BO2) blended with additives at different concentrations

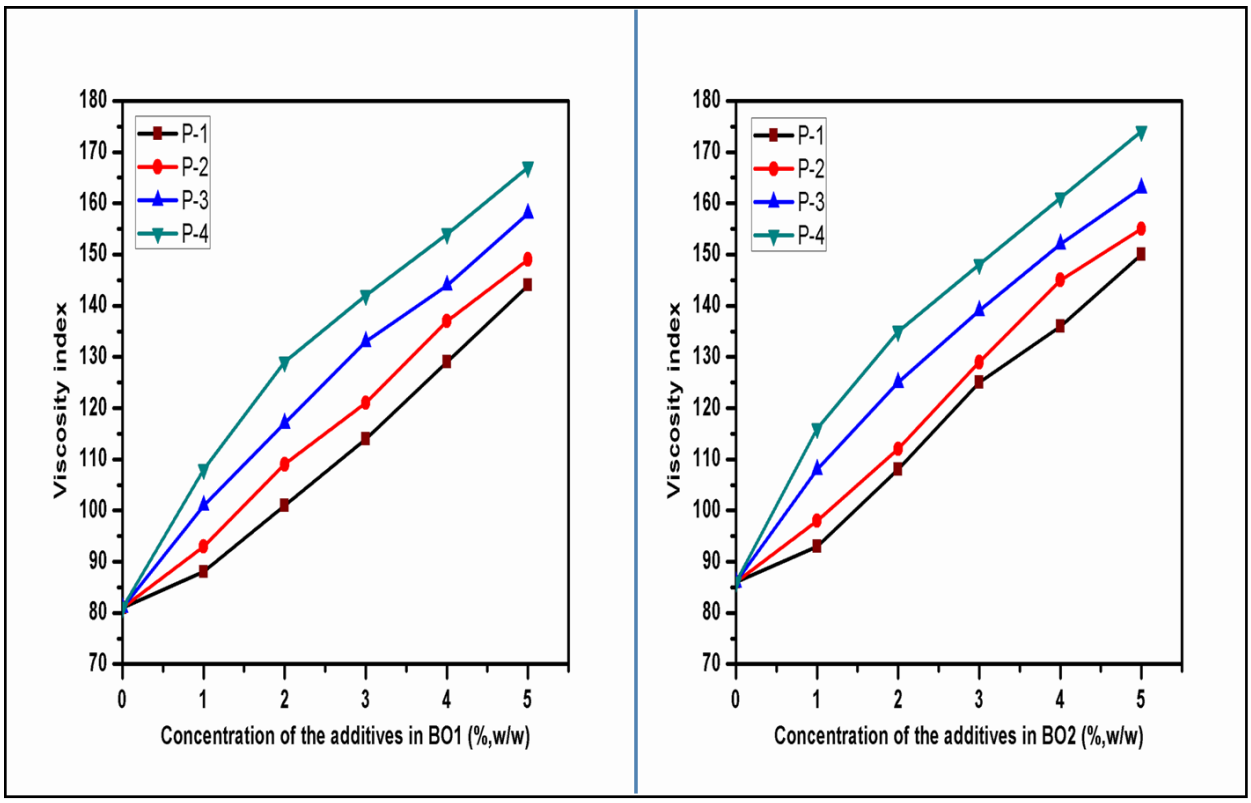

Figure 2.4.20: Photomicrograph of: (a). untreated base oil BO1 (b). BO1 blended with additive P-1 (4%, w/w) (c). BO1 blended with additive P-2 (4%, w/w) (d). BO1 blended with additive P-3 (4%, w/w) (e). BO1 blended with additive P-4 (4%, w/w)

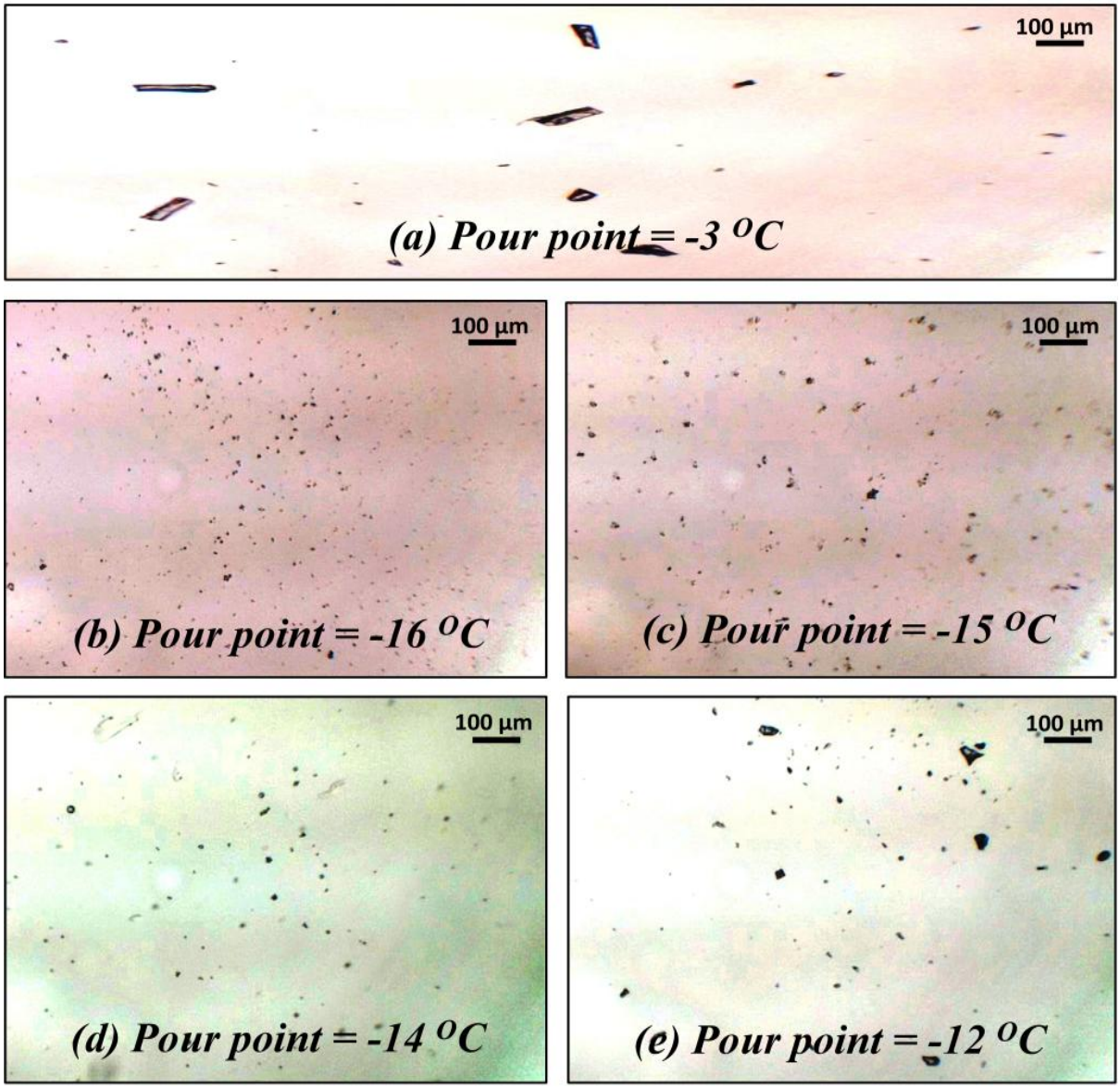

Figure 2.4.21: Degradation of the additives measured in the SBD test